

# Entropic uncertainty measure for fluctuations in two-level electron-phonon models

E. Majerníková<sup>1,2,a</sup>, V. Majerník<sup>3</sup>, and S. Shpyrko<sup>1</sup>

<sup>1</sup> Department of Theoretical Physics, Palacký University, Tr. 17. listopadu 50, 77207 Olomouc, Czech Republic

<sup>2</sup> Institute of Physics, Slovak Academy of Sciences, Dúbravská cesta, 84 228 Bratislava, Slovak Republic

<sup>3</sup> Institute of Mathematics, Slovak Academy of Sciences, Štefánikova 49, 814 73 Bratislava, Slovak Republic

Received 22 September 2003

Published online 20 April 2004 – © EDP Sciences, Società Italiana di Fisica, Springer-Verlag 2004

**Abstract.** Two-level electron-phonon systems with reflection symmetry linearly coupled to one or two phonon modes (exciton and  $E \otimes (b_1 + b_2)$  Jahn-Teller model) exhibit strong enhancement of quantum fluctuations of the phonon coordinates and momenta due to the complex interplay of quantum fluctuations and nonlinearities inherent to the models. We show that for the complex correlated quantum fluctuations of the anisotropic two-level systems the Shannon entropies of phonon coordinate and momentum and their sum yield their proper global description. On the other hand, the variance measures of the Heisenberg uncertainties suffer from several shortcomings to provide proper description of the fluctuations. Wave functions, related entropies and variances were determined by direct numerical simulations. Illustrative variational calculations were performed to demonstrate the effect on an analytically tractable exciton model.

**PACS.** 71.38.-k Polarons and electron-phonon interactions – 63.70.+h Statistical mechanics of lattice vibrations and displacive phase transitions – 02.50.-r Probability theory, stochastic processes and statistics

## 1 Introduction

In spite of long-term research, various aspects of the theory of polarons with Holstein coupling in two-level local and lattice models related with quantum fluctuations and phase transitions belong to systematically studied topics in the current literature up to the present time [1–7].

The class of two-level electron-phonon models with linear coupling to one or two phonon modes represent several important physical systems: excitons, dimers, Jahn-Teller (JT) systems (rotationally symmetric  $E \otimes e$  and reflection symmetric  $E \otimes (b_1 + b_2)$  JT model with broken rotational symmetry). Especially, interest in the literature is growing in the JT models [2,3]; There is the experimental evidence of related structural phase transition in some spatially anisotropic complex structures (perovskites, fullerenes, manganites [3, 8–10]).

In two-level electron-phonon models strong enhancement of fluctuations of phonon coordinates and momenta as well as of their product in certain ranges of model parameters were reported by several authors from both numerical simulations and analytical (e.g. variational) approaches: Feinberg et al. [11] in a model of an exciton, Borghi et al. [12] in the Holstein-Hubbard two-level model, Morawitz et al. [13] in the Holstein-Peierls model.

Recently, we have investigated numerically and variationally the interplay of quantum fluctuations and nonlinearity inherent to the two-level models in the ground state of the  $E \otimes (b_1 + b_2)$  molecular (local) JT model [14] and the respective lattice JT model [15]. Corresponding Hamiltonians contain a hidden nonlinearity due to the reflection symmetry (the nonlinearity appears explicitly under an appropriate unitary transformation; see Section 2 and discussion in our recent papers [14,15]). There is to elucidate the terminology related to quantum fluctuations and the nonlinearity parameters used there [14] and in the present paper: quantum fluctuations are measured by the ratio of the phonon frequency and the classical parameter of electron-phonon interaction,  $\Omega/\alpha = 1/\sqrt{2\mu}$ , while the nonlinearity parameter is the quantum tunneling strength between the levels,  $\beta/\alpha = \chi$ . In the plane  $\mu, \chi$  ( $\mu = \alpha^2/2\Omega^2$ ) there occur quantum fluctuations  $\sim \Omega$  and  $\sim \chi$ . The ground state in the phase plane  $\mu, \chi$  exhibits regions of dominance of either selftrapping (classical) ( $\mu > 1, \chi < 1$ ) or tunneling (quantum) parameters ( $\mu < 1, \chi > 1$ ) and regions where the classical and quantum regions mix together ( $\mu < 1, \chi < 1$  or  $\mu > 1, \chi > 1$ ). For  $\mu < 1$ , formation of both the selftrapping and tunneling “phases” is suppressed by the quantum fluctuations  $\propto \Omega$ . The parameter of nonlinearity  $\chi$  and phonon frequency  $\Omega$  are both of quantum origin so that global

<sup>a</sup> e-mail: majere@prfnw.upol.cz

quantum fluctuations mix the fluctuations due to nonlinearity close to the border of two regions at  $\chi \sim 1$  and the quantum fluctuations  $\sim \Omega$ .

Numerical approach to the two-level exciton and JT models in consideration in comparison with variational approaches bring understanding of the nature of mixing of quantum fluctuations with the nonlinearities: since the coherent phonon subsystem does not conserve the number of phonons the upper level participates in the distribution of phonons even in the ground state. This manifests itself by the appearance of additional reflective extrema of the ground state wave function [16,17]. The distance between its extrema is related to the displacement of the coherent phonons and is involved into the dispersion measure of the wave function and of its Fourier transform [18–20]. This displacement, i.e. the measure of the polaron self-localization, though suppressed by quantum fluctuations, is of *classical origin*. This is the source of difficulties with the justification of the moment (variance) characterization of fluctuations in the case of the wave function with the presence of the additional reflection maximum. As it is known, in the case of multipeak wave functions, the variances for the coordinate and/or momentum of related wave functions, as well as for other non-commuting observables do not stand for appropriate uncertainty measures [18–22], since these uncertainty measures strongly involve distance between the peaks.

Another serious shortcoming arises when we switch from one- to two- or more phonon system, like Jahn-Teller systems are (generally – to a system with several non-independent variables). In this case the moment-related uncertainty measures are not good even for one-peak distribution, since the width of the distribution given by the variances is a width in a particular direction chosen arbitrarily, and cannot stand for actual “width” of a distribution.

In these cases the Shannon entropies of the probability density functions assigned to such wave functions were used as alternative uncertainty measures of the conjugated coordinates. The “entropies” of any probabilistic distribution are well-known to eliminate effectively both the distance between peaks in the multipeak distributions and the said “anisotropy” of the distribution in the space of random variables since they contain in their expressions only functions of probability distributions, rather than values of a random trial, as in momentum measures.

For references, we shall briefly summarize necessary notions: in the probability theory there are two main types of the integral uncertainty measure assigned to an observable, the moment and entropic ones [23]. Due to existence of these uncertainty measures two types of uncertainty relations (UR) for two non-commuting observables can be introduced: (i) the Heisenberg (variance) UR and (ii) the entropic UR. While the moment (variance) UR is expressed as the *product* of the variances of two noncommuting observables  $A$  and  $B$ , the entropic UR is given by the *sum* of their Shannon entropies. For a continuous observable  $A$  with the density of probability distribution  $p(x)$

the (differential) entropy of  $A$  is defined as [24]

$$H_c = - \int p(x) \log p(x) dx.$$

The entropic uncertainty relation for the coordinate and momentum of a quantum system described by its normalized function  $\psi(x)$  is represented by the inequality [18,25]

$$S_x + S_p \geq S_{xp}, \quad (1)$$

where  $S_x$  and  $S_p$  are the entropies of its coordinate and momentum probability distributions

$$S_x = - \int_{-\infty}^{\infty} |\psi(x)|^2 \log |\psi(x)|^2 dx \quad (2)$$

and

$$S_p = - \int_{-\infty}^{\infty} |\varphi(p)|^2 \log |\varphi(p)|^2 dp, \quad (3)$$

respectively, and  $\varphi(p)$  is the Fourier transform of the wave function  $\psi(x)$  and  $S_{xp}$  represents the lower bound of the right-hand side of the inequality (1).

It has been found by Białynicki-Birula and Mycielski [25] that the lower bound  $S_{xp} = 1 + \log \pi$  for the harmonic oscillator represents the minimal lower bound for any quantum system with one pair of non-commuting observables. Therefore, the sum of coordinate and momentum entropies of the arbitrary quantum system is ( $\hbar = 1$ )

$$S_x + S_p \geq 1 + \log \pi. \quad (4)$$

This relation is an entropic counterpart of the famous Heisenberg principle formulated by means of variances:  $\Delta x \Delta p \geq 1/2$ .

We note that the entropy as a measure of uncertainty and the entropic uncertainty relations are widely used in quantum optics [22,26] being useful for systems with more complex structure of photon coherent states (e.g., Schrödinger cat coherent states).

In Section 2, two standard two-level electron-phonon models with linear electron-phonon coupling are described as prototype models for which the entropic uncertainty principle represents the adequate measure of the fluctuations. The nonlinearity hidden in the (initially linear) two-level phonon Hamiltonians is revealed after appropriate diagonalization of the problem with respect to the electronic subspace.

In Section 3 we determine by direct numerical simulations the wave functions of one-phonon exciton model for a range of model parameters. From those, we determine and compare the quantum fluctuations as functions of the effective interaction  $\mu$  described by means of the Shannon entropies of the phonon coordinate and momentum on one hand and by means of their variances on the other hand. Comparison of the sum of the coordinate and momentum Shannon entropies and the corresponding product of the

variances clearly puts forward the former as more adequate measure of the quantum fluctuations in certain parameter region than the latter one.

Our approach is consequently based on numerical simulations, because variational treatments based on squeezed coherent states or their linear combinations were generally found to underestimate quantum fluctuations: (i) they underestimate quantum fluctuations originating from finite phonon frequency [27,28] for weak couplings; (ii) The fluctuations due to the nonlinearity in the crossover region are strongly coupled with the fluctuations (i). Therefore, in the region close to the crossover there appear discontinuities which are artefacts of variational approaches (similar to those of the adiabatic approximation).

In Section 3.1 leaning upon variational treatment of the exciton model we present results of simple analytical estimations of quantum fluctuations (both entropic uncertainties and variances) to illustrate the failure of variational methods. However, in a small range of the phase plane we can identify the effect of the classical displacement in the Heisenberg variances and their product by means of variational method.

Similar investigations for the two-mode phonon  $E \otimes (b_1^\dagger + b_2)$  Jahn-Teller model (which differs from the model of Section 3 by the presence of phonon assistance in the tunneling term and, consequently, the existence of additional mode correlations effects) are presented in Section 4.

## 2 Model Hamiltonians

For the model of interest let us consider the two-level reflection symmetric electron-phonon system with linear (Holstein) coupling to one or two phonon modes

$$H = \sum_{i=1}^{N=1,2} \Omega(b_i^\dagger b_i + 1/2) + \alpha(b_1^\dagger + b_1)\sigma_z - \beta\Lambda\sigma_x, \quad (5)$$

where the Pauli matrices  $\sigma_x, \sigma_z$  represent electron density operators in the pseudospin notation,  $\sigma_z = \frac{1}{2}(c_2^\dagger c_2 - c_1^\dagger c_1)$ ,  $\sigma_x = \frac{1}{2}(c_1^\dagger c_2 + c_2^\dagger c_1)$  with  $I = c_1^\dagger c_1 + c_2^\dagger c_2$  as the unit operator [15].

For the case of coupling to one phonon mode,  $N = 1$ , we take  $\Lambda = 1$  and two-level Hamiltonian (5) represents an exciton or a dimer with tunneling between the levels with the tunneling amplitude  $\beta$ . The prototype model has been handled both variationally and numerically by many authors in its local and extended version [11, 16, 17, 29]. In the case of the coupling with two phonon modes,  $N = 2$ , the second term with  $\Lambda = b_2^\dagger + b_2$  represents phonon-assisted tunneling between the levels (the flip-flop rate is proportional to the value of phonon-2 coordinate, i.e. an additional ‘‘phonon pumping’’ occurs in distinction to the one-phonon case). The special case  $\alpha = \beta$  represents standard  $E \otimes e$  Jahn-Teller Hamiltonian with rotational symmetry [10, 30–33]. The phonon 1-mode is antisymmetric and the 2-mode is symmetric against the reflection.

The case  $\alpha \neq \beta$  is the reflection symmetric  $E \otimes (b_1 + b_2)$  Jahn-Teller Hamiltonian recently investigated variationally and numerically [14, 15].

The reflection symmetry of the Hamiltonians (5) involves a nonlinearity which reveals itself explicitly after performing Fulton-Gouterman unitary transformation (Fulton et al. [34], Shore et al. [16]):

$$H_{FG} = UHU^{-1} = \Omega \sum_{i=1}^{N=1,2} (b_i^\dagger b_i + 1/2) + \alpha(b_1^\dagger + b_1)I \mp \beta\Lambda \exp(i\pi b_1^\dagger b_1), \quad (6)$$

where  $U = \frac{1}{\sqrt{2}} \begin{pmatrix} 1, & G \\ 1, & -G \end{pmatrix}$ ,  $G = \exp(i\pi b_1^\dagger b_1)$  is the reflection operator in the phonon space,  $G(b_1^\dagger + b_1) = -(b_1^\dagger + b_1)G$ , which performs virtual coupling of the levels by phonons 1 mediating the electron (Rabi) oscillations between them.

The transformation (6) diagonalizes (5) in the electronic subspace yielding however a strong nonlinearity in the phonon subspace (term containing  $\beta$ ) which otherwise was hidden in the initial Hamiltonian (5). The unitary transformation left us with purely phonon Hamiltonian (6) while electrons were excluded. All further consideration will be performed for the ground state which for both models is given by the upper sign in the transformed Hamiltonian (6).

The competition of quantum fluctuations ( $\Omega$ ), the self-localization ( $\alpha$ ) and the phonon assisted tunneling ( $\beta$ ) in (6) determines regions of dominance of said effects for different sets of the parameters. In the next sections, we shall analyze these regions by numerical simulations of the models (6).

## 3 Exciton: coupling to a single phonon mode

The main purpose of this and of the next section is to show that for the considered prototype models the entropic uncertainties and the entropic uncertainty principle represent adequate measures of quantum fluctuations instead of the moment (variance) Heisenberg ones.

The exciton model, including respective wave functions, has been previously intensively investigated by many authors. Here we shall confine ourselves to essential points needed for our purposes.

The results of the numerical simulations of the ground state wave functions of the model (6) for  $\Lambda = 1$ , i.e. of one-mode diagonal coupling case, are shown in Figure 1. The parameter of the effective interaction  $\mu = \alpha^2/2\Omega^2$  is the measure of the competition between the classical polaron selflocalization due to the interaction of the energy  $\alpha^2/2\Omega$  (e.g., Holstein [35]) and of the quantum fluctuations of the energy  $\Omega$ . Parameter  $\beta/\Omega$  is the measure of the competition between the quantum term of the tunneling  $\beta$  and quantum fluctuations  $\Omega$ . Wave functions shown in Figure 1 illustrate the effects of the interplay between these parameters affecting the population of the phonons

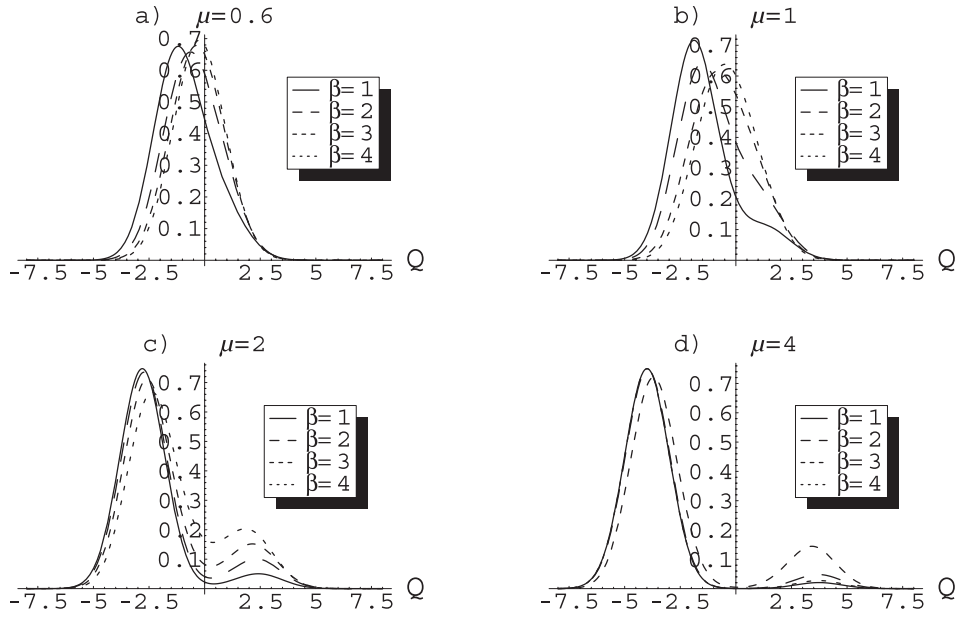


**Fig. 1.** Ground state wave functions of one-phonon model parametrized by  $\beta$  and  $\mu$ ,  $\mu = 0.6$  (a);  $\mu = 1$  (b);  $\mu = 2$  (c);  $\mu = 4$  (d);  $\Omega = 1$ .

on both levels. One can see that the most prominent deviations from the one-peak wave function occur for large  $\mu$ ; For moderate  $\mu$  and  $\beta$ , ( $\Omega = 1$ ) the wavefunctions also tend to exhibit variations from almost-Gaussian shapes. These features are consistent with non-conservation of the number of the coherent phonons involved. They inspired the variational approach based on linear combination via a variational parameter of two harmonic oscillators related to both levels [16,17]. Numerical evaluation of the ground state (Fig. 2) illustrates smooth decrease of the energy as function of  $\mu$  indicating a smeared crossover region. The sharp transition line between two regions resulting from the competition of two interactions ( $\mu$  and  $\beta$ ) is known to be an artefact of the adiabatic approximation and often of inadequate variational approaches. In the quantum treatment the crossover line is smoothed over the region of a width  $\approx \Omega$  of the phonon energy.

These regions are analogous to the “selftrapping dominated” and the “tunneling dominated” regions for the  $E \otimes (b_1 + b_2)$  model [14,15] (see the next section). In the weak coupling region,  $\mu < 1$ , the formation of the “ordered phases” (either selftrapping- or tunneling-dominated) is suppressed by the quantum fluctuations  $\sim \Omega$  as well as in the model of Section 4.

Corresponding to the above described reasons for qualifying the quantum deviation from the harmonic oscillator (Gaussian) behaviour we evaluated numerically (Fig. 3a) the left-hand side of the Shannon uncertainty relation, the sum of entropies  $S_Q + S_P$  (4) (here,  $Q$  and  $P$  are the coordinate and momentum of the phonon). The product of variances  $\sqrt{\Delta Q^2 \Delta P^2}$  containing explicitly the displacement (distance between the peaks) is shown in Figure 3b. Both approaches, the variance and the Shannon entropy ones, can be compared to illustrate their different physical content. Close to the line of equal effective coupling and

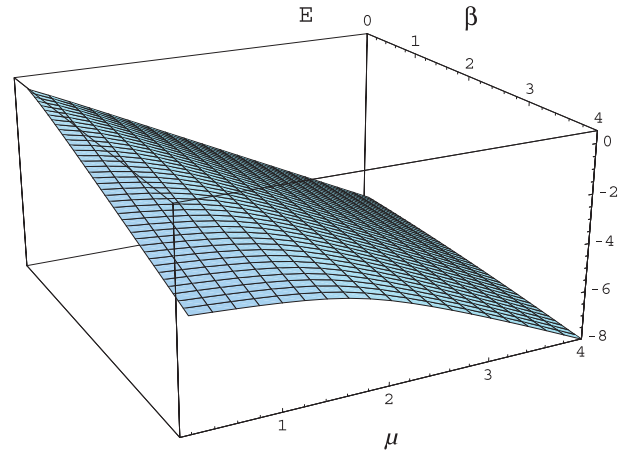


**Fig. 2.** Ground state energy in the plane  $\mu$  and  $\beta$ .

the tunneling strength  $2\mu = \beta$  the extremum of the sum of Shannon entropies manifests itself markedly. The pictures of related wave functions attribute this extremum by the maximal overlapping (tunneling) of the contributions of both levels (Fig. 1b). With growing polaron selflocalization  $\mu$  the quantum fluctuations are suppressed and both oscillator parts tend to separate, see Figure 3a for large  $\mu$ . The harmonic oscillator value  $1 + \log \pi = 2.14473$  is recovered in both regions around the crossover region: in the limits of large  $\mu$  or, on the contrary, for large  $\beta$  and small or moderate  $\mu$  (less than some critical value on the crossover line).

The product of variances  $\sqrt{\Delta Q^2 \Delta P^2}$  at Figure 3b shows similar behaviour except for large  $\mu$ , where it therefore accounts for the growing distance of the peaks of the wave functions with  $\mu$ , Figure 1d. This distance as a

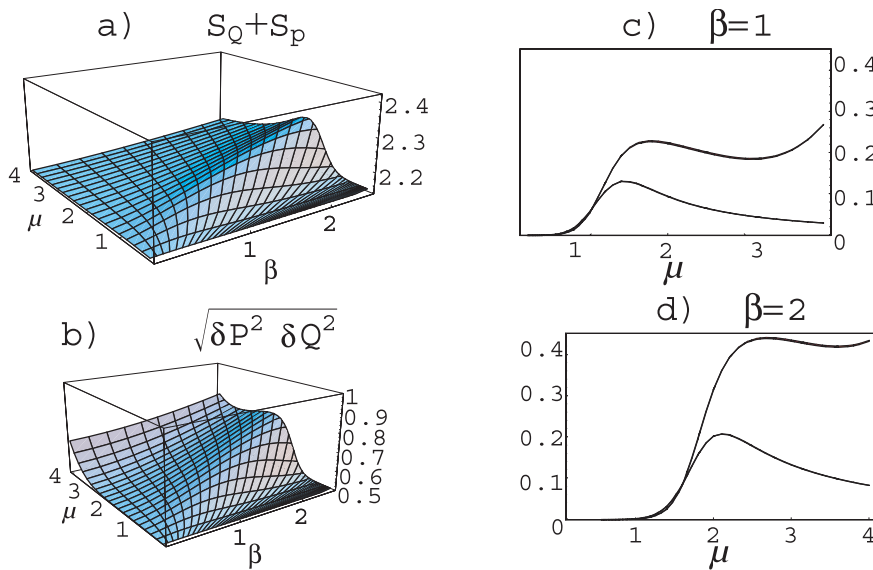


**Fig. 3.** Sum of entropies  $S_Q + S_P$  (a) vs. product of variances  $\sqrt{\Delta Q^2 \Delta P^2}$  (b) for one-phonon model;  $\Omega = 1$ . Product of variances (upper curves) and exponent of the sum of entropies (lower curves) shifted to the respective minimal values  $1/2$  and  $1 + \log \pi$ , respectively, for  $\beta = 1$  (c),  $\beta = 2$  (d). Illustration of the growing product of variances as functions of the classical parameter  $\mu$  when compared with the sum of entropies.

function of a *classical parameter*  $\mu$  is a measure of the non-linearity since it maps the position of the reflection peak. In the limit of small  $\mu$ ,  $\sqrt{\Delta Q^2 \Delta P^2}$  tends to the harmonic oscillator value 0.5.

The range of maximum fluctuations in the plane  $\mu, \beta$  (Fig. 3) separates the quantum fluctuation dominated region of the harmonic oscillator ( $2\mu < \beta$ ) and the self-trapping dominated region ( $2\mu > \beta$ ). Although both uncertainty measures yield similar behaviour in the crossover range showing the common increase of fluctuations, and in the tunnelling region where the wavefunctions indeed converge to an oscillator, the quantitative information beyond the crossover region is different in the selftrapping region. Enhancement of fluctuations reported by the variance uncertainty picture in the selftrapping region point merely on the *classical* contribution related to the displacement so that *it fails to play a role of a measure of quantum fluctuations*. This shortcoming is effectively eliminated by the Shannon entropic relations which thus help to extract purely quantum effects manifested in our case in the strongly non-Gaussian behaviour of single peaks.

Figures 3c, d compare crosssections of both Figures 3a, b as functions of  $\mu$  for different  $\beta$ . The entropies and variances plotted on one graph (both shifted by the oscillatory values of corresponding quantities) illustrate the difference of two approaches: the Heisenberg product of variances with increasing  $\mu$  (upper curves in Figs. 3c, d) is growing while the sum of entropies tends to the oscillator value as expected. (For quantitative comparison we should plot rather exponents of the sum of entropies than the entropies; this becomes clear if we remind of the famous Einstein relation between entropies and fluctuations  $\exp(S) \sim \Delta X^2$ , but the difference between them is almost inappreciable.)

In the next section we shall illustrate these considerations by means of analytical calculations of both measures based upon a variational fitting of wavefunctions.

The enhancement of quantum fluctuations for the exciton model have been found by Feinberg, et al. [11] by numerical calculation of the moment (variance) uncertainties and their product as functions of parameters  $\alpha^2 \equiv 2\mu$  and  $\lambda \equiv 2\mu/\beta$ . For given  $\alpha$ , their dependence on  $\lambda$  means in our notations the dependence on  $1/\beta$ . Let us note that these fluctuations are related to the competition of the parameters  $\mu$  and of the nonlinearity parameter  $\beta$ , i.e. related to a crossover between the selftrapping dominated and the tunneling dominated regions. However, the undesirable presence of the classical nonlinearity manifests itself in the dependence of  $\sqrt{\Delta Q^2 \Delta P^2}$  on  $\mu$  due to the competition between the parameters  $\alpha$  and  $\Omega$ . Namely, it becomes obvious when the product of variances is depicted as a function of  $\alpha^2 \equiv 2\mu$  as in Figure 3.

### 3.1 Analytical illustration: variational approach

Though the variational approaches based on squeezed coherent states are not suitable for description of quantum fluctuations we will apply them for evaluations of fluctuations of a simple exciton model. We can use them for demonstration of the effect of interest (i.e. of the involvement of the displacement in the moment uncertainties product in contrast to its entropic counterpart). We will use variational approach with two squeezed coherent harmonic oscillators linearly combined by a variational parameter (12) in accordance with the concept initiated by Shore and Sander [16]. However, this illustrative analytics is valid only if the maxima of the wave function are well separated from each other (small overlapping), i.e.

for strong coupling (large  $\mu$ ). This is just the region of the most prominent difference of both said concepts of the uncertainty measure.

Phonon variational wave function for the two-level model with one phonon mode ( $\Lambda = 1$ ) (6) as solution to the Fulton-Gouterman equation [17, 29, 34]

$$\begin{aligned} H_{FG}^{(p)} \phi^{(p)} &= [\Omega (b^\dagger b + 1/2) + \alpha (b^\dagger + b) - p\beta G] \phi^{(p)} \\ &= E^{(p)} \phi^{(p)}, \\ p &= \pm 1 \end{aligned} \quad (7)$$

for the ground state ( $p = 1$ ) can be chosen in the form [16, 17]:

$$|\psi^{(1)}\rangle = \frac{1}{\sqrt{C}} (1 + \eta G) |\phi^{(1)}\rangle, \quad (8)$$

where  $G = \exp(i\pi b^\dagger b)$  is reflection operator in the phonon space,  $G|\phi^{(1)}\rangle = |\phi^{(2)}\rangle G$ , and

$$|\phi^{(1,2)}(\gamma, r)\rangle = D(\pm\gamma) S(r) |0\rangle. \quad (9)$$

The indices 1(2) pertain to the lower (upper) level. The functions  $D(\gamma)$  and  $S(r)$  are generators of displacement and squeezing depending on the variational parameters:

$$\begin{aligned} D(\gamma) &= \exp[\gamma(b^\dagger - b)], \\ S(r) &= \exp[r(b^{\dagger 2} - b^2)] \end{aligned} \quad (10)$$

acting on the phonon vacuum  $|0\rangle$ . The normalization constant in (8) is  $C = 1 + \eta^2 + 2\eta \exp[-2\gamma^2 \exp(-4r)]$ . Wave function (8)–(10) represents two squeezed displaced harmonic oscillators combined by a variational parameter  $\eta$  (compare with Fig. 1).

Variational parameters of the displacement  $\gamma$ , squeezing  $r$  and the parameter of admixture of the reflection part of the upper level  $\eta$  can be determined by minimalization of the Hamiltonian (7) averaged over (8):

$$\begin{aligned} \langle H \rangle &= \frac{1}{2} \cosh 4r + \frac{1}{C} \gamma^2 (1 + \eta^2 - 2\eta \exp(-8r) \exp(-2\tilde{\gamma}^2)) \\ &+ \frac{2\alpha}{C} (1 - \eta^2) \gamma - \frac{\beta}{C} ((1 + \eta^2) \exp(-2\tilde{\gamma}^2) + 2\eta), \\ \tilde{\gamma} &\equiv \gamma \exp(-2r). \end{aligned} \quad (11)$$

(The parameters are scaled so that  $\Omega = 1$ .)

It is worth noting that variational approaches of varying degree of reliability combined with unitary transformations are widely used for electron-phonon systems [11–17, 28, 29, 31, 36]. Comparison of different variational Ansatzes for one-phonon two-level system was performed e.g. by Shore et al. [16], Sonnek et al. [17] and for  $E \otimes (b_1 + b_2)$  model by the present authors [14].

Let us evaluate variances of the phonon coordinate  $Q = (b^\dagger + b)/\sqrt{2}$  and momentum  $P = (b^\dagger - b)/i\sqrt{2}$ ,  $(\Delta Q)^2 = \langle Q^2 \rangle - \langle Q \rangle^2$ ,  $(\Delta P)^2 = \langle P^2 \rangle - \langle P \rangle^2$ , where we average over the states (8–10).

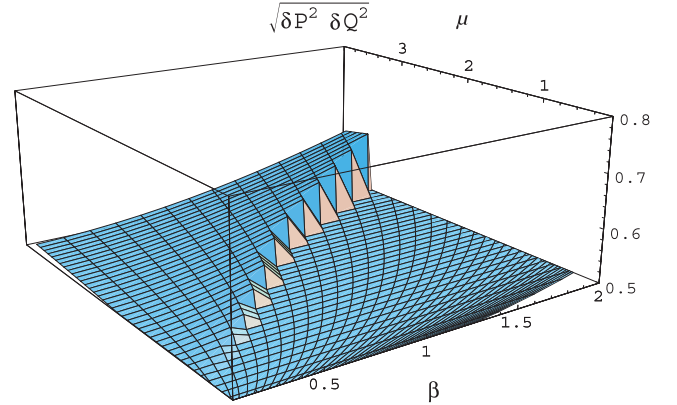


**Fig. 4.** Product of variances  $\sqrt{\Delta P^2 \Delta Q^2}$  calculated from the variational approach of Section 3.1 (12–13). Compared to Figure 3 the fluctuations are completely suppressed on the right part of the figure.

We get

$$(\Delta Q)^2 = \frac{1}{2} \exp(4r) \left( 1 + 8\eta \tilde{\gamma}^2 \frac{2\eta + (1 + \eta^2) \exp(-2\tilde{\gamma}^2)}{(1 + \eta^2 + 2\eta \exp(-2\tilde{\gamma}^2))^2} \right), \quad (12)$$

$$(\Delta P)^2 = \frac{1}{2} \exp(-4r) \left( 1 - 8\eta \tilde{\gamma}^2 \frac{\exp(-2\tilde{\gamma}^2)}{1 + \eta^2 + 2\eta \exp(-2\tilde{\gamma}^2)} \right). \quad (13)$$

For large  $\gamma$ , the product of variances can be estimated by

$$(\Delta Q)^2 (\Delta P)^2 \simeq \frac{1}{4} \left( 1 + \frac{16\eta^2}{(1 + \eta^2)^2} \tilde{\gamma}^2 \right), \quad (14)$$

where  $\tilde{\gamma}$  is defined by (11). From (12, 13) and (14) it is obvious that the anomalous enhancement of fluctuations is due to the contribution of the classical displacement (reduced by squeezing)  $\tilde{\gamma}$  and is mediated by the reflection parameter  $\eta$ . If  $\eta = 0$ , we are left with a single harmonic oscillator as expected.

It is easy to perform simple illustrative analytical estimations for the values of variational parameters as functions of the model parameters. Assuming in (11)  $r, \eta$  small, we get an approximate equation for  $\gamma$  setting  $\partial \langle H \rangle / \partial \gamma = 0$  (compare similar procedure in the recent paper [14]),

$$\gamma (1 + 2\beta \exp(-2\tilde{\gamma}^2)) = -\alpha, \quad (15)$$

(from similar considerations the expression for  $\eta$  can also be found).

Figure 4 illustrates results of the variational approach for the Heisenberg product of variances: in comparison with Figure 3b, there occurs a complete suppression of fluctuations in the tunneling region  $\sim 2\mu < \beta$ . Instead of the smooth crossover there occurs sharp discontinuity which is an artefact because of underestimation of the fluctuations  $\sim \Omega$  similar to that of adiabatic approximation. In the selftrapping region,  $\sim 2\mu > \beta$ , the increase is evidently caused by the classical contribution because quantum fluctuations tend to disappear in the classical limit of the strong coupling.



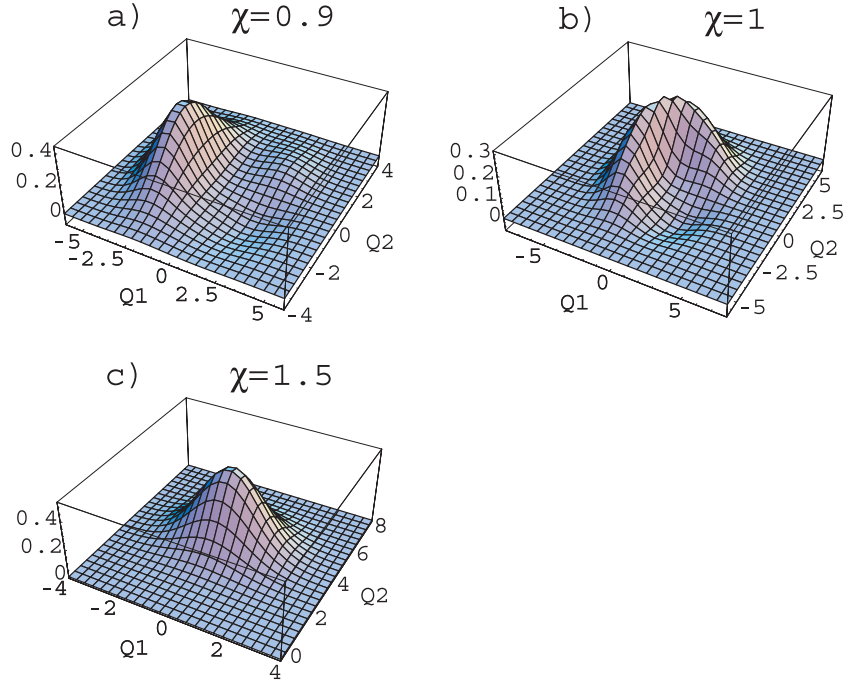


**Fig. 5.** The two-phonon numerical ground state wave functions at  $\mu = 2$  and  $\chi = 0.9$  (a),  $\chi = 1$  (b) and  $\chi = 1.5$  (c).

To illustrate the advantages of the entropic uncertainty relation over the moment Heisenberg ones for our case we calculate approximately the expressions for the Shannon entropies of coordinate and momentum for the ansatz (8), (9). This can be easily done analytically if  $\eta \ll 1$  and  $\gamma \gg \exp(2r)$  (last condition meaning that two peaks of the wavefunction are well separated and almost do not overlap).

For the entropies  $S_Q$  and  $S_P$  (2-3) with (8-10) we get

$$S_Q = \frac{1}{2}(1 + \log \pi) + \log(1 + \eta^2) + 2r - \frac{\eta^2}{1 + \eta^2} \log(\eta^2) + O(\varepsilon, \eta^3), \quad (16)$$

$$S_P = \frac{1}{2}(1 + \log \pi) - 2r - \frac{\eta^2}{(1 + \eta^2)^2} + O(\varepsilon, \eta^3), \quad (17)$$

$$\varepsilon \equiv \exp(-2\tilde{\gamma}^2).$$

From (16, 17)

$$S_Q + S_P = 1 + \log \pi + \log(1 + \eta^2) - \frac{\eta^2}{(1 + \eta^2)^2} - \frac{\eta^2}{1 + \eta^2} \log(\eta^2) + O(\varepsilon, \eta^3). \quad (18)$$

For  $\eta = 0$ , equation (18) reduces to the single oscillator value  $1 + \log \pi$  as expected. Contrasting (18) with (14) we see that entropy uncertainty relations are weakly dependent of the displacement  $\tilde{\gamma}$  and contain as the main contribution owing to the parameter  $\eta$  originating from the nonlinear effect due to coupling between levels.

#### 4 Interplay between quantum fluctuations and nonlinearity in $E \otimes (b_1 + b_2)$ Jahn-Teller model

Quantum ground state of  $E \otimes (b_1 + b_2)$  Jahn-Teller reflection symmetric model (a degenerate electron level coupled with two phonon modes, one symmetric and one antisymmetric against the reflection) has been investigated in our recent papers for the one site [14] and lattice [15] case. Let us expound the main results relevant to clarify the origin of quantum fluctuations of interest.

Exact numerical simulations of the solution to the Hamiltonian (6) with  $\Lambda = b_1^4 + b_2$  yield the ground state wave functions depicted in Figures 5a, b, c (in the coordinate representation in the space  $(Q_1 \otimes Q_2)$ ), in terms of the parameters  $\mu = \alpha^2/2\Omega^2$  and  $\chi = \beta/\alpha$  for three characteristic regions [14]. The two-phonon ground state wave functions for the case of phonon-assisted tunneling exhibit evident mixing of the phonon-1 wave functions related to the lower and excited levels at  $\chi < 1$ , Figure 5a. Each of the levels refers to one of two competing minima of the effective potential composed of  $\alpha$ - and  $\beta$ -components, as described below, Figure 6. The mixing due to the two mode correlation is pronounced most effectively in the region of the dominant quantum fluctuations  $\Omega$ ,  $\mu < 1$ ,  $\chi \simeq 1$  [14]. At  $\chi > 1$ , the prominent peak refers to a harmonic oscillator of the dominant potential well  $\beta$  related to the selflocalized state of an electron oscillating between the levels (Fig. 5c). Because of the phonon-2 assistance there occurs a smeared continuous crossover from the regime of selflocalization (Fig. 5a) towards the tunnelling regime (Fig. 5c) through the intermediate picture close to the  $E \otimes e$  Jahn-Teller case (Fig. 5b).

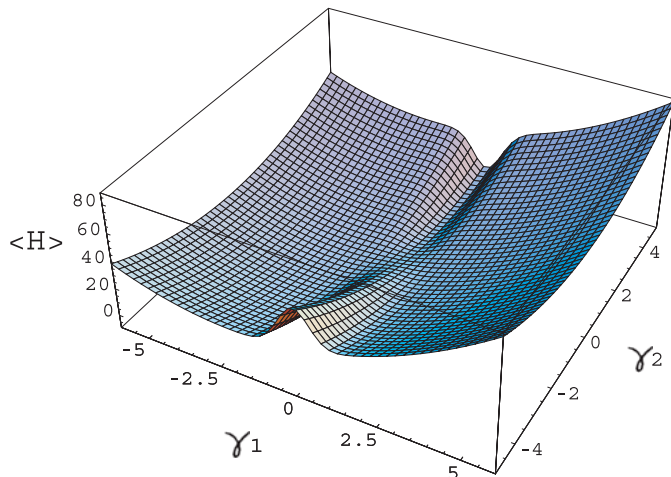


**Fig. 6.** Effective potential in the plane  $\gamma_1, \gamma_2$  containing several competing minima for  $\mu = 2, \chi = 1.5$ . For this values of the parameters the narrow (tunneling) minimum  $\gamma_1 \simeq 0, \gamma_2 > 0$  dominates. For  $\chi < 1$  the broad minimum at  $\gamma_1 < 0, \gamma_2 \simeq 0$  would dominate (the selftrapping).

In spite of the limitations of variational approaches (their failure close to the crossover between two regimes, underestimation of quantum fluctuations) they provide useful insight into the behaviour of the ground state. The complex interplay of the nonlinear and quantum effects has been analyzed by numerical simulations and compared with results of various variational treatments [14]. We note that the variational wave functions with the admixture of the excited symmetric phonon mode (phonons-2) we proposed recently [14] for the ground state showed significant improvement of the agreement with numerical simulation results especially for strong e-ph couplings  $\mu$ . The topology of the effective variational potential, Figure 6 (Hamiltonian (6) averaged over trial functions depending on a set of variational parameters) is controlled by several model parameters; it plausibly can acquire two or more competing minima referring to the ground state with a possible admixture of the side minimum referring to the excited state [14]. As a result, two regions of the ground state appear according to which one of two local minima of the potential dominates; generically two regions are recognized – with either dominating selftrapping ( $\chi < 1$ ) or tunneling ( $\chi > 1$ ). The existence of selftrapping dominated vs. tunneling dominated regions results from complex competition of two nonlinearly coupled coherent phonon modes ( $\beta$ -term in (6)). Let us note, that the order parameters for the selftrapping dominated “phase” is the displacement  $\langle b_1^\dagger + b_1 \rangle \sim Q_1$  and for the tunneling dominated “phase”  $\langle b_2^\dagger + b_2 \rangle \sim Q_2$ . These features are analogous for both local [14] and a generalized lattice [15]  $E \otimes (b_1 + b_2)$  JT model.

The additional phonon-2 assistance of the tunneling with non-conservation of the number of the phonons 2 implies their selfconsistent behaviour and creation of a corresponding potential well which develops proportionally to the interaction strength  $\beta$  (Fig. 6). At the same time the correlation of both phonon modes is involved

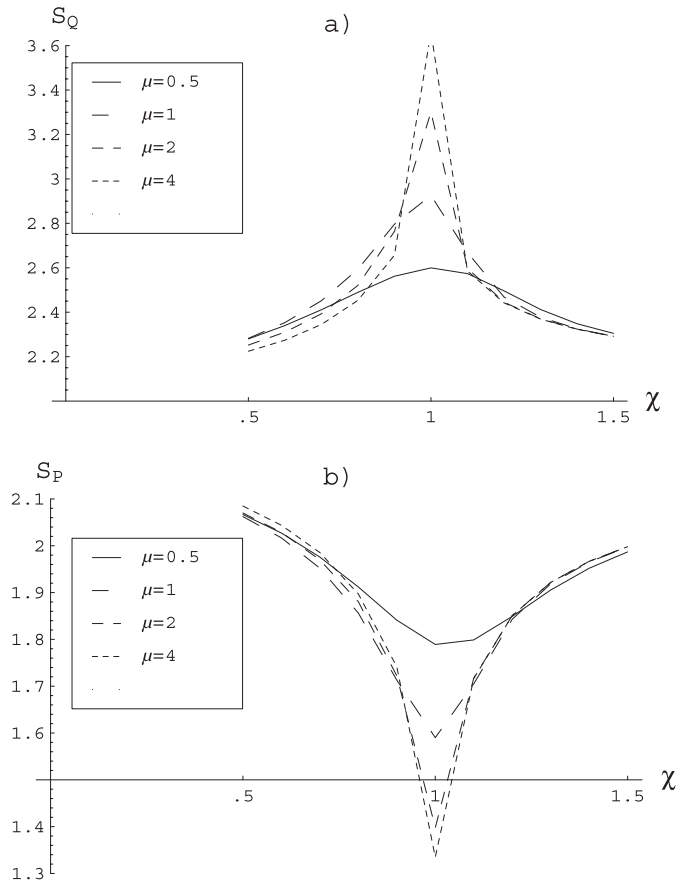


**Fig. 7.** Shannon entropies  $S_Q$  (a) and  $S_P$  (b) as functions of  $\chi$  and  $\mu$ .

(last term of (6)) via the multiple (Rabi) tunneling mediated by the mode 1 as a source of the nonlinearity. The nonlinearity significantly enhances the quantum fluctuations in the region of maximal tunneling between the levels [14]. Competition of the terms responsible for selftrapping and phonon-assisted tunneling between the levels resulting in formation of two ground state regions is accompanied by increased anomalous quantum fluctuations in the crossover region. There is to be emphasized that, similarly to the case of  $\Lambda = 1$  (Fig. 2), there exists no sharp transition line in the ground state of the energy in the phase diagram. The transition region is smeared by a width of the phonon frequency  $\Omega$ . Sharp transition line occurs rather as a well known artefact of some variational approaches and of the adiabatic approximation [16].

In order to describe the quantum fluctuations resulting from the complex interplay of the above described contributions we have numerically evaluated the Shannon entropies  $S_Q, S_P$  (Figs. 7a, b) and their sum  $S_Q + S_P$  (Fig. 8a) as functions of  $\mu$  and  $\chi$ . Here  $Q \equiv \{Q_1, Q_2\}$  and  $P \equiv \{P_1, P_2\}$  and all integrations are meant in the two-dimensional space  $Q_1 \times Q_2$ , resp.  $P_1 \times P_2$ .

In the weak coupling region,  $\mu = \alpha^2/2\Omega^2 \leq 1$ , formation of the “phases” at  $\chi < 1$  and  $\chi > 1$  is greatly reduced because of the fluctuations  $\Omega$  and strong correlations between the phonon modes (Fig. 8a). For large  $\mu$  the extrema at  $\chi \simeq 1$  get sharper but remain



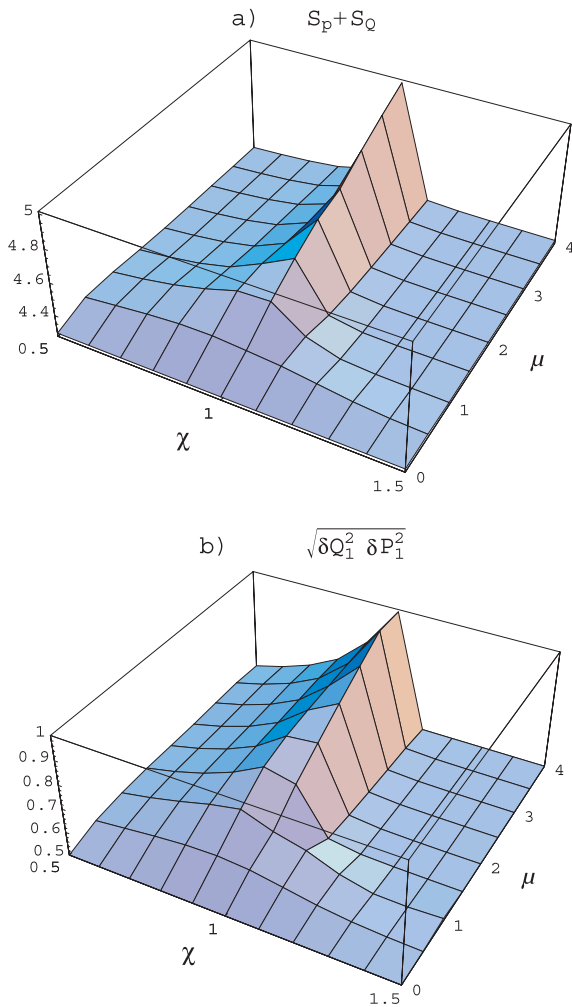


**Fig. 8.** Sum of entropies  $S_Q + S_P$  in the plane  $\chi, \mu$ . The lower bound corresponds to the two harmonic oscillators value  $2(1 + \log \pi)$  (a); Product of variances  $\sqrt{\Delta Q_1^2 \Delta P_1^2}$  in the plane  $\chi, \mu$  (b). The difference of two figures is not so well pronounced as on its one-dimensional counterpart Figure 3, but for better insight the reader is referred to following Figure 9 with pertaining crosssections.

non-singular due to the finite (although small) quantum fluctuations  $\Omega$ . The obvious asymmetry of the sum of entropies  $S_Q + S_P$  as a function of  $\chi$  comes from the fluctuations of the  $\chi > 1$  “phase”. In the limit of large  $\chi$ , both uncertainties, entropic and momentum ones, tend to their values corresponding to two harmonic oscillators,  $2(1 + \log \pi) = 4.28946$  and  $0.5$ , respectively (Figs. 8a, b or 9a, c). This resembles much the tunneling dominated region of one-phonon model (Sect. 3) with the single exception that the tunneling region is spread for all  $\mu$  because of the pronounced crossover enhanced by phonon-2 pumping.

Numerical result for the product  $\sqrt{\Delta Q_1^2 \Delta P_1^2}$  as function of  $\mu$  and  $\chi$  is shown in Figures 8b and 9b, d. The contour plots of Figure 8 presented in Figure 10 help visualizing their difference, namely (i) the classical contribution of the displacement growing with the coupling  $\mu$  to the Heisenberg product, Figure 10b, and (ii) prevention of

formation of the selftrapping dominated and the tunneling dominated regions in the weak coupling region  $\mu < 1$ . Except for the region  $\mu \geq 2$  the difference between Figures 8a and 8b is seen not so clear as on the corresponding Figures 3a, b for one-phonon model. However it can be easily traced if one compares the corresponding crosssections along  $\chi$  and  $\mu$  axes, visualised in Figures 9a–d. In particular, of main interest for the application of suggested alternative measure are regions of large  $\mu$  close to  $\chi \simeq 1$  and of  $\chi \leq 1$  where the wavefunctions exhibit pronounced multipeak structure, as seen from Figures 5a, b.

The region of maximum in Figures 8a, b at  $\mu \simeq 1$  refers to the crossover between the quantum fluctuation dominated region  $\mu < 1$  and the selflocalization dominated region  $\mu > 1$ . Namely, at  $\mu \sim 1$  there occurs a crossover from two correlated oscillators towards two independent oscillators, which is visualized in Figure 8a. These two independent oscillators (see wavefunctions in Fig. 5a) refer to the complexity of the classical (i.e. adiabatic limit) potential and the entropic relations handle them accurately marking this region as a “classical” one with close to two-oscillator value  $2(1 + \log \pi)$ . On the contrary, the variances in the left-hand side of the Heisenberg uncertainty relation (Fig. 4b) continue increasing for small  $\chi$  with growing  $\mu$ , but apparently weaker than in the one-phonon case of Section 3. In the two-phonon case the separation of two peaks of the wave function in the selftrapping region is much less pronounced than in the one-phonon case, which is seen also from the moderate increase of the product of variances at Figures 8b, 9c, 10b, for  $\chi < 1$  in comparison with the corresponding one-phonon case at Figure 3b.

## 5 Conclusion

Two-level electron-phonon systems with one (exciton) and two ( $E \otimes (b_1 + b_2)$  Jahn-Teller model) phonon modes exhibit reflection symmetry as the source of a hidden nonlinearity which reveals explicitly by appropriate unitary diagonalization (Fulton-Gouterman transformation (6)) of the Hamiltonian. This diagonalization (i) excludes electrons leaving us with solely phonon Hamiltonian (exact decoupling in electron subspace), (ii) reveals quantum correlation of phonon modes in the case of two-phonon model. As a consequence, related phonon wave functions exhibit multipeak, i.e. essentially non-Gaussian structure even in the ground state. Besides this “topological” anisotropy, additional anisotropy appears in two-phonon model due to the correlation of the modes. Resulting complex topology of the ground state implies appearance of two regions in the phase plane  $\mu, \chi$  or  $\mu, \beta$ : the selftrapping dominated region for  $\chi < 1$  or  $2\mu > \beta$  and the tunneling dominated region for  $\chi > 1$  or  $2\mu < \beta$  respectively, for both models due to competition of two antagonistic (classical selftrapping and quantum tunneling [14, 15]) interactions in the Hamiltonian (terms with  $\alpha$  and  $\beta$  in (5)). The enhancement of fluctuations close to the crossover between these two regions behaves in analogy with the corresponding items of the theory of critical phenomena but appears smoothed by the finite phonon frequency  $\Omega$ . Namely, quantum fluctuations due to finite phonon frequency  $\Omega$  prevent formation

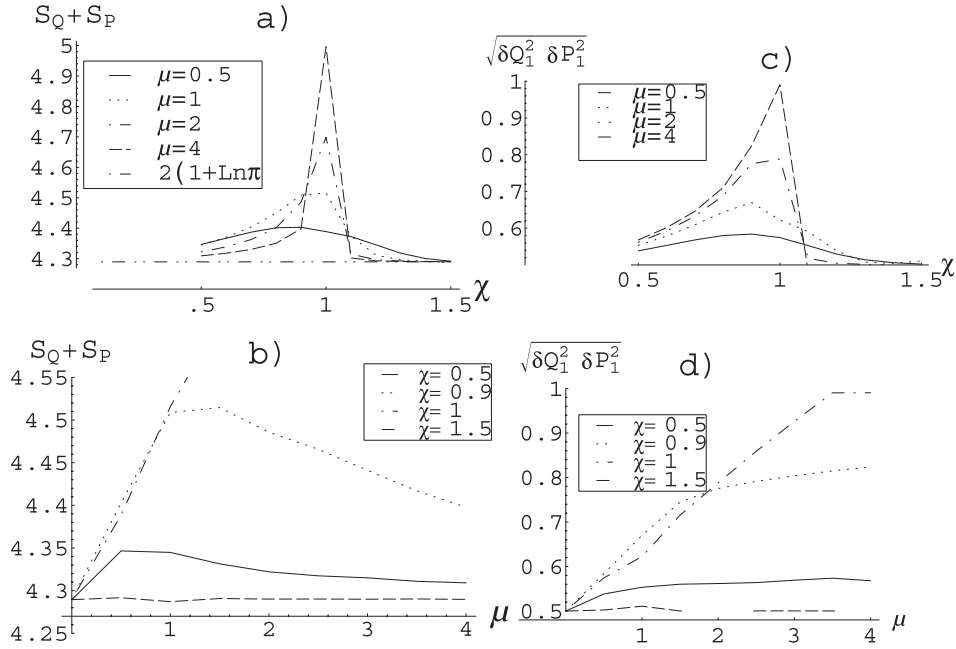


**Fig. 9.** Cross-section of the sum of entropies at Figure 8a,  $S_Q + S_P$  as a function of  $\chi$  for various  $\mu$  (a). The same as a function of  $\mu$  for several  $\chi$  (b). Cross-section of the product of variances  $\sqrt{\Delta Q_1^2 \Delta P_1^2}$  at Figure 8b as a function of  $\chi$  for various  $\mu$  (c). The same as a function of  $\mu$  for various  $\chi$  (d).

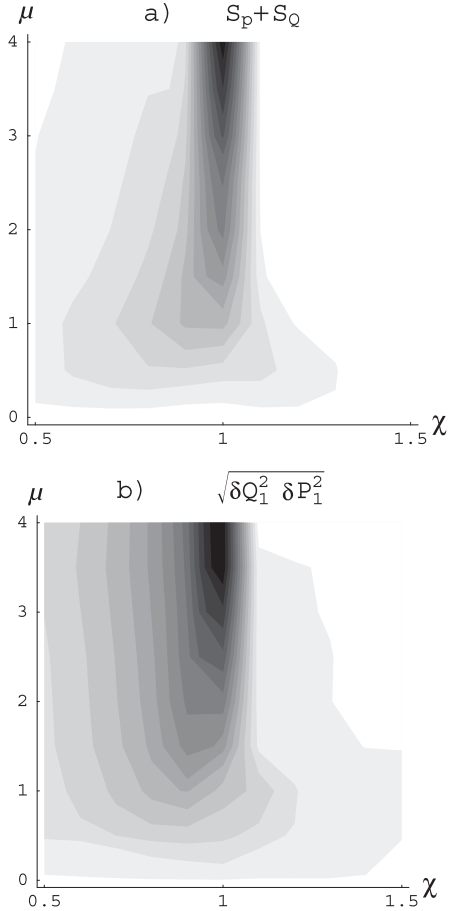


**Fig. 10.** Contour plots of the sum of entropies of Figure 8a (a) and of the product of variances of Figure 8b (b).

of the ordered “phases” in the region of weak coupling  $\mu < 1$  in the phase plane  $\mu, \beta$  or  $\mu, \chi$ . The interplay of the classical and quantum terms yields complex interplay (mixing) of quantum fluctuations  $\propto \Omega$  and nonlinear fluctuations  $\propto \chi$ .

The moment and entropic uncertainty measures represent two classes of characteristics used in the probability theory in order to describe quantitatively the spreading of the probability distribution for an observable. The uncertainty principle in quantum mechanics leans essentially on the probabilistic interpretation of the wavefunction and can be thus formulated in a twofold fashion – in the form of either moment (variance) or entropic uncertainty relation.

The aim of this paper was to show that for certain parameter region the appropriate quantitative measure of phonon quantum fluctuations of the systems in consideration could be the entropic uncertainty measures rather than the moment measures (variances) used in the Heisenberg uncertainty relation. We have compared results of numerical simulations for both types of measures and show that the latter exhibits serious shortcomings in description of the global fluctuations of such systems.

Namely, Heisenberg uncertainty relations impose the measure under integration ( $Q_i^2$ , resp.  $P_i^2$ ) which is noninvariant in the space of variables – both translationally and rotationally. Hence there are two sources of the disqualification of the Heisenberg variances, both resulting from the anisotropy of wavefunctions caused by the reflection symmetry of considered models: (i) former non-invariance has its consequences in difficulties describing the multi-peak distributions, and (ii) latter one – when trying to judge about two or more strongly correlated variables.

Problem of characterization of quantum fluctuations by variances for a system of two correlated oscillators is much more subtle than for one oscillator of Section 3. In addition to the problems imposed by multipeak distributions a serious difficulty arises if several coupled variables are involved (in our case – two strongly correlated phonon oscillators). If for one-mode case (and for the probability distribution with a single peak)  $\langle \Delta X^2 \rangle$  could stand for an effective “width” of the distribution function, in many-variable case it represents only an average “width” in the  $X$ -direction, that is the measure under the integral is not the best choice since it is strongly affected by, e.g., basis rotation. As an example just consider a squeezed correlated two-phonon trial function [14] of the general form  $\exp(-\sum_{i,j=1,2} a_{ij} x_i x_j)$  representing an arbitrarily turned ellipsoid in  $(x_1, x_2)$ -plane. To judge about the “width” of such distribution in terms of variances one should therefore consider rather tensor quantities representing the “width” of the distribution for every direction [37].

The entropic measure, on the contrary, does not suffer from this shortcoming. It presents a handy characteristics of essentially scalar character which can be applied for any number of coupled variables, but is not affected by the basis rotation. This holds generally for a measure which suggests taking an average of some function of the distribution itself (averaging of  $\log P(x)$ , as for Shannon entropy considered here, or generalized entropic measures, like, for example, Rényi entropy [21]).

Similar problems arise, e.g. in quantum optics, at the description of fluctuations of the photon coherent Schrödinger cat states and photon multimode correlated systems (see, e.g. Ohya et al. [26] and Bužek [22] and references therein). The entropic uncertainty relations are commonly recognized there as a good tool for handling fluctuations of quantum origin.

The support from the Grant Agency of the Czech Republic of our project No. 202/01/1450 is highly acknowledged. We thank also the grant agency VEGA (No. 1/0251/03) for partial support.

## References

1. *Polarons and bipolarons in high- $T_c$  superconductors and related materials*, edited by E.K.H. Salje, A.S. Alexandrov, W.Y. Liang (Cambridge University Press, 1995)
2. M.D. Kaplan, B.G. Vekhter, *Cooperative phenomena in Jahn-Teller crystals*, edited by V.P. Fackler (Plenum, New York and London, 1995)
3. G.M. Zhao, K. Conder, H. Keller, K.A. Müller in *Electrons and Vibrations in Solids and Finite Systems (Jahn-Teller Effect)*, Berlin 1996, edited by H.J. Schultz, U. Scherz (R. Oldenbourg Verlag, München, 1997), p. 537
4. E.V.L. de Mello, J. Ranninger, Phys. Rev. B **55**, 14872 (1997)
5. J.K. Freericks, M. Jarell, D.J. Scalapino, Phys. Rev. B **48**, 6302 (1993)
6. A.J. Millis, R. Mueller, B. Shraiman, Phys. Rev. B **54**, 5389 (1996); A.J. Millis, R. Mueller, B. Shraiman, Phys. Rev. B **54**, 5405 (1996)
7. V.A. Ivanov, M.A. Smondyrev, J.T. Devreese, Phys. Rev. B **66**, 134519 (2002)
8. O. Gunnarson, Phys. Rev. Lett. **74**, 1875 (1995); O. Gunnarson, Rev. Mod. Phys. **69**, 575 (1997)
9. K.A. Müller, J. Supercond. **12**, 3 (1999)
10. M.C.M. O’Brien, C.C. Chancey, Am. J. Phys. **61**, 688 (1993)
11. D. Feinberg, S. Ciuchi, F. de Pasquale, Int. J. Mod. Phys. B **4**, 1317 (1990)
12. G.-P. Borghi, A. Girlando, A. Painelli, J. Voit, Europhys. Lett. **34**, 127 (1996)
13. H. Morawitz, P. Reineker, V.Z. Kresin, J. Lumin. **76&77**, 567 (1998)
14. E. Majerníková, S. Shpyrko, J. Phys.: Condens. Matter **15**, 2137 (2003)
15. E. Majerníková, J. Riedel, S. Shpyrko, Phys. Rev. B **65**, 174305 (2002)
16. H.B. Shore, L.M. Sander, Phys. Rev. B **7**, 4537 (1973).
17. M. Sonnek, T. Frank, M. Wagner, Phys. Rev. B **49**, 15637 (1994)
18. V. Majerník, L. Richterek, Eur. J. Phys. **18** 79 (1997)
19. V. Majerník, E. Majerníková, J. Phys. A **35**, 5751 (2002)
20. D.A. Trifonov, J. Math. Phys. **35**, 2297 (1994)
21. V. Majerník, E. Majerníková, S. Shpyrko, Central Europ. J. Phys. **3**, 393 (2003)
22. V. Bužek, C.H. Keitel, P.L. Knight, Phys. Rev. A **51**, 2575 (1995) and references therein
23. J.B.M. Uffink, *Measures of uncertainty and the uncertainty principle*, Ph.D. Thesis, University of Utrecht, 1990
24. S. Guisasu, *Information Theory with Application* (McGraw-Hill, New York, 1977)
25. I. Białyński-Birula, J. Mycielski, Comm. Math. Phys. **44**, 129 (1975); W. Beckner, Ann. Math. **102**, 159 (1957); B. Mamojka, Intern. J. Theor. Phys. **11**, 7 (1974)
26. M. Ohya, D. Petz, *Quantum Entropy and its Use* (Springer, Berlin-New York, 1993)
27. E. Fradkin, J.E. Hirsch, Phys. Rev. Lett. **49**, 402 (1982)
28. H. Zheng, D. Feinberg, M. Avignon, Phys. Rev. B **39**, 9405 (1989)
29. U. Herfort, M. Wagner, J. Phys.: Condens. Matter **13**, 3297 (2001)
30. H. Barentzen, O.E. Polansky, Chem. Phys. Lett. **49**, 121 (1977)
31. C.F. Lo, Phys. Rev. A **43**, 5127 (1991)
32. H. Eiermann, M. Wagner, J. Chem. Phys. **96**, 4509 (1992)
33. H. Barentzen, Eur. Phys. J. B **24**, 197 (2001)
34. R.L. Fulton, M. Gouterman, J. Chem. Phys. **35**, 1059 (1961)
35. T. Holstein, Ann. Phys. (N.Y.) **8**, 325 (1959)
36. M. Wagner, *Unitary Transformations in Solid State Physics* (North Holland, Amsterdam, 1986)
37. It is worth noting that the problem mentioned arises in more general context, namely within the realm of descriptive statistics. The conventional parametric statistics which is based on momenta estimation often fails to represent adequately the characteristics of nonuniform data and sometimes it leaves the scene in favour to the “nonparametric statistics” As the simplest example, consider the ordinary mean (first momentum)  $\int xp(x)dx$  of a strongly asymmetric distribution function. Within the nonparametric statistics in order to characterize intuitive notion of the “distribution center” it is common to use the median, or 1/2-quantile instead of the mean value